



The formation of three-grain junctions during solidification. Part I: observations

Marian B. Holness¹ · A. C. Fowler^{2,3}

Received: 4 August 2021 / Accepted: 15 April 2022 / Published online: 11 May 2022
© The Author(s) 2022

Abstract

The thermodynamic equilibrium dihedral angle at grain junctions in crystalline rocks is set by the grain boundary interfacial surface energies, but the long times required to attain equilibrium mean that the observed dihedral angles in igneous rocks are generally set by the kinetics of crystallisation. We distinguish three types of augite–plagioclase–plagioclase dihedral angle in mafic igneous rocks. In the first, augite grows in the pores of a pre-existing plagioclase framework accompanied by little to no inwards-growth of the plagioclase pore walls. In the second, the plagioclase pore walls grow inwards simultaneously with the augite, and the dihedral angle is generally larger than the original angle at which the two plagioclase grains impinged except when the impingement angle itself is large. The first type is seen in rapidly crystallised rocks, whereas the second is observed in slowly cooled rocks. The third type is highly asymmetric and resembles (and so we call) an eagle's beak: it is only seen in slowly cooled rocks. It is common in gabbroic cumulates, and is also present in strongly orthocumulate troctolites. Using the mode of interstitial phases to calculate the amount of interstitial liquid present in a series of mafic cumulates from the Rum and Skaergaard layered intrusions, we show that the asymmetry of three-grain junctions in troctolites increases as the rocks progress from adcumulate to orthocumulate (i.e. as the olivine–plagioclase crystal mush becomes more liquid-rich), with eagles' beaks becoming the dominant three-grain junction geometry for troctolitic mushes containing ~ 12 vol.% interstitial material (corresponding to ~ 30 vol.% liquid in the mush). The geometry of three-grain junctions in mafic rocks is thus a function not only of cooling rate, but also of the progression along the liquid line of descent during fractionation. The first two types of junction are formed in relatively primitive liquids, during which the crystal mushes on the margins of the solidifying magma body are formed predominantly of plagioclase and olivine, whereas the eagle's beak geometry occurs once augite forms an important component of the crystal framework in the accumulating mush, either because it is a framework-forming primocryst phase or because it grows from highly abundant interstitial liquid.

Keywords Magma crystallisation · Dihedral angle · Eagles' beaks

Introduction

Recent work has demonstrated that the detailed geometry of grain junctions formed by two plagioclase grains and one grain of augite in fully solidified igneous rocks preserves valuable information about the time-scales of solidification and cooling (Holness et al. 2012a, b; Holness 2015). In general, the geometry of three-grain junctions in igneous rocks ranges from that formed during solidification as grains impinge, to that expected for textural equilibrium. The former is a function of the relative rates of growth of the three impinging mineral grains and, for augite–plagioclase–plagioclase junctions, is a sensitive function of cooling rate (Holness 2015). The latter is controlled by the balancing of grain boundary energies after the three-grain junction has

Communicated by Timothy L. Grove.

✉ A. C. Fowler
fowler@maths.ox.ac.uk

¹ Department of Earth Science, University of Cambridge, Downing Street, Cambridge CB2 3EQ, UK

² Mathematics Applications Consortium for Science and Industry, Department of Mathematics and Statistics, University of Limerick, Limerick, Ireland

³ Oxford Centre for Industrial and Applied Mathematics, Mathematical Institute, University of Oxford, Oxford, UK

formed: the establishment of the equilibrium geometry of the three-grain junction is the first step in the process of subsolidus textural equilibration (Voll 1961), followed by modification of the entire grain boundary network to create a granular microstructure if the temperature (and diffusion rates) remain sufficiently high. The rarity of granular microstructures in igneous rocks demonstrates that complete subsolidus textural equilibration is seldom achieved: it is generally approached only in fine-grained chill zones surrounding kilometre-scale intrusions, and is localised to monomineralic regions in intrusion interiors (Fig. 1a; Holness et al. 2012a). Furthermore, that most three-grain junctions involving two different phases in plutonic rocks preserve a geometry essentially unmodified from that created during solidification suggests that even the earliest stages of subsolidus textural equilibration do not take place in most plutonic rocks.

In this contribution, we focus on three-grain junctions formed during solidification, for which we do not yet have a

quantitative model describing how the relative growth rates of the different grains, and the order in which they impinge, control the shape of the resultant junction. Such a model is the first step towards predicting the population of dihedral angles formed during solidification, necessary to fully quantify the temporal information preserved in igneous rocks. We concentrate on augite–plagioclase–plagioclase junctions in systems with low undercooling, in which crystal growth is controlled by attachment kinetics, resulting in compact grains (rather than those with high undercooling, in which diffusion-limited growth results in dendritic or other non-compact forms), and show that the geometry of augite–plagioclase–plagioclase three-grain junctions can be categorised into three types: which type ends up being dominant depends on the cooling rate during solidification and the extent to which augite is a framework-forming phase. In the companion paper, we describe a simple theoretical model to account for our observations.

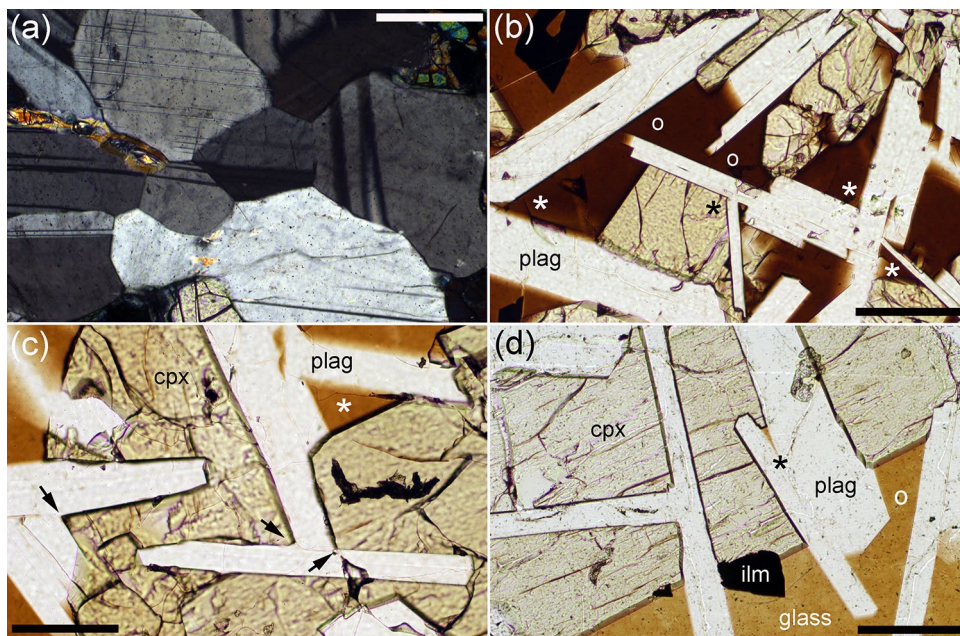


Fig. 1 **a** Huntly Gabbro, Aberdeenshire, viewed under crossed polars. The plagioclase in this field of view has lost the original tabular growth shape, with a localised granular microstructure expected for subsolidus textural equilibration. Scale bar is 1 mm long. **b** Sample collected in 1976 from 145.3 ft depth below the surface of the Kilauea Iki lava lake photographed under plane polarised light. Note the framework of tabular plagioclase grains with augite growing in the spaces between. In this image only one three-grain junction has been created (black asterisk). The white asterisks show nascent three-grain junctions where the plagioclase grains have already impinged, and the white circles denote potential three-grain junctions where the two plagioclase grains have not yet impinged. Scale bar is 200 μ m long. **c** sample collected 143.3 ft below the surface of the Kilauea Iki lava lake in 1976, viewed in plane polarised light. Solidification has progressed to the point where many three-grain junctions are formed. The three arrowed junctions show two where the augite has

infiltrated and pseudomorphed the space formed by two impinging plagioclase tablets: note that the central arrowed junction shows a slightly rounded morphology, created by some growth of plagioclase during the filling of the melt-filled pore corner. The asterisk shows a melt-filled pore created by the impingement of two plagioclase tablets, which is partly infilled by augite. Scale bar is 1 mm long. **d** The later stages of solidification of the crust of the Kilauea Iki lava lake involve grain impingement and the formation of three-grain junctions: at the left of the image are two well-formed augite–plagioclase–plagioclase junctions. The asterisk shows a narrow melt-filled pore defined by two impinged plagioclase grains, with augite growing into the remaining liquid. The white circle on the right shows a nascent three-grain junction where the two plagioclase grains have not yet impinged. This second junction is likely to develop into an eagle's beak. Scale bar is 200 μ m long

Previous work

The population of true, 3D, augite–plagioclase–plagioclase dihedral angles in a texturally equilibrated rock, has a median value, Θ_{cpp} , of 109° , and a standard deviation (caused by anisotropy of interfacial energies) of $\sim 10^\circ$ (Holness et al. 2012a). The geometry of augite–plagioclase–plagioclase three-grain junctions created during solidification of mafic magma is generally far from that expected for textural equilibrium, with median values of the dihedral angle population significantly lower than 109° , and standard deviations greater than 10° . Θ_{cpp} varies smoothly across unfractionated dykes and sills (Holness et al. 2012b, 2013), and is constant over large stretches of stratigraphy in fractionated bodies, such as layered intrusions, in which it changes in a step-wise manner with changes in the number of phases on the liquidus of the bulk magma (Holness et al. 2013). The variation in Θ_{cpp} can be straightforwardly linked to the variation of cooling rate in unfractionated bodies, with the highest values in the slowly-cooled centre and low values on the rapidly-cooled margins (Holness 2014). In layered mafic intrusions, the step-wise changes in Θ_{cpp} are argued to be a result of step-wise changes in the contribution of latent heat to the overall enthalpy budget as the number of liquidus phases changes (Holness et al. 2013; Morse 2011).

Based on the observation that plagioclase nucleates early in mafic magmas, forming a framework of tabular grains (Philpotts et al. 1998, 1999; Philpotts and Dickson 2000) in which augite fills the spaces (Figs. 1b–d), Holness (2015) argued that the underlying control on the median value of the population of dihedral angles formed during solidification is the varying response of different plagioclase growth faces to changes in the cooling rate. Slow cooling favours relatively more growth on the (010) faces and, since most of the augite–plagioclase–plagioclase dihedral angles in mafic rocks are created by the meeting of 2 plagioclase (010) growth faces (Holness 2014, 2015), increasing amounts of growth on these faces during the closure of the melt-filled pore increases the final dihedral angle.

Accordingly, due to imperceptible amounts of inwards-growth of the plagioclase forming the pore walls in rapidly-cooled dolerites, three-grain junctions in rapidly-cooled rocks form by the (near-) perfect pseudomorphing by augite of original melt-filled pores formed by the impingement of planar sided plagioclase grains (Figs. 1c, d, 2a). In samples in which the framework-forming plagioclase grains were oriented randomly, if augite filled every such junction, the resultant median dihedral angle would be 60° . However, due to the inhibition of nucleation and growth in small pores (caused by the greater supersaturation required (Cahn 1980) and slower mass transport in low permeability regions), the narrower junctions tend to be filled with late-stage material

such as K-feldspar, quartz or mesostasis (Fig. 2b). This under-representation of the narrower angles in the distribution means that the lowest observed median dihedral angle, Θ_{cpp} , associated with minimal amounts of growth of the pore walls, is $\sim 78^\circ$ (Holness et al. 2012b). The random orientation of the plagioclase grains means that the standard deviation of this population of dihedral angles is high ($\sim 30^\circ$ for populations of true 3D angles measured using a universal stage). Junctions of this first type are seen in dolerites that crystallised in less than 10 years (Holness et al. 2012b). They are also found in the slowly cooled, highly evolved ferro-gabbros of the Skaergaard Intrusion in which the minimal inwards-growth of the plagioclase pore walls is attributed to the cessation of significant plagioclase growth from the highly evolved interstitial liquid (Holness et al. 2017).

In more slowly cooled dolerites and gabbros (those that took longer than ~ 10 years to crystallise; Holness et al. 2012b), three-grain junctions are characterised by a generally symmetrical curvature of the plagioclase–augite boundaries immediately adjacent to the junction (Fig. 2c), denoting some inwards-growth of the plagioclase walls of the melt-filled pore. As pointed out by Holness (2015), the more the plagioclase walls grow, the higher the dihedral angle of the resultant junction. In natural examples, the median value of the dihedral angle population can reach $\sim 100^\circ$ in samples with this second type of geometry, and the standard deviation of the population decreases with increasing values of Θ_{cpp} .

A closer examination of three-grain junction geometry in mafic plutonic rocks shows that these two types of junction form only part of the story. In many gabbroic cumulates, three-grain junctions are notably asymmetric, with the two plagioclase–augite grain boundaries having the same sense of curvature, similar to that of an eagle's beak (Fig. 2d). Rocks with abundant junctions of this type tend to have high values of Θ_{cpp} , with a corresponding low standard deviation. There is no published discussion of this third type of junction, and it does not fit with the current understanding of the controls on three-grain geometries in mafic rocks. Here we show, using observations of natural samples, that the development of this third type, the eagle's beak, is critically dependent on the extent to which the plagioclase crystal framework is established before significant growth of augite occurs.

Choice of samples

For a detailed examination of the effects of the original impingement angle on the final dihedral angle, we chose three dolerites from unfractionated sills that have already been subjected to close microstructural examination. We chose two samples from the Portal Peak sill, Antarctica, with

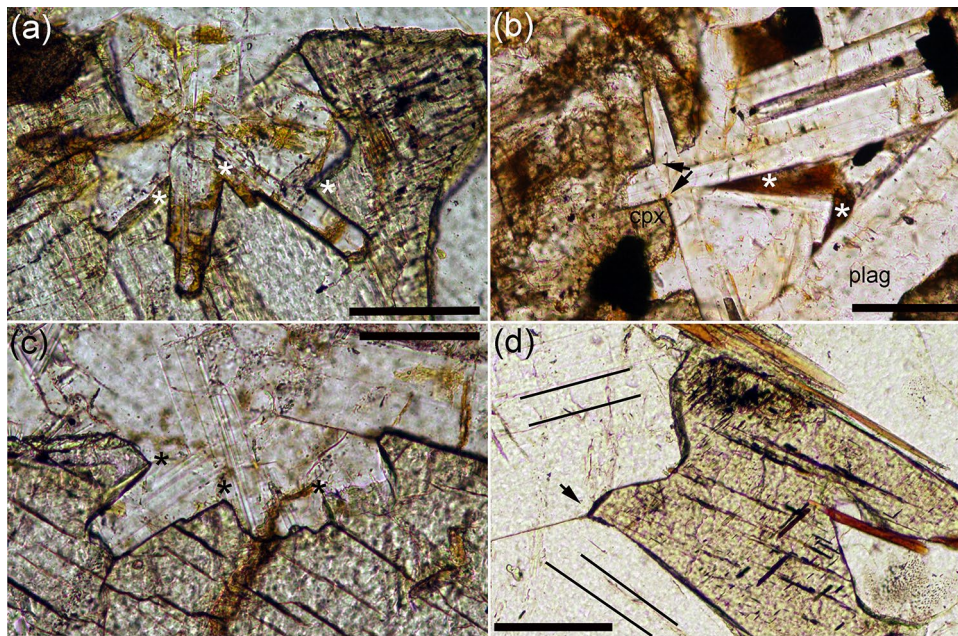


Fig. 2 **a** Sample 87–95, from the margin of the 128 m thick Portal Peak sill, Antarctica (previously described by Holness et al. 2012b), photographed under plane polarised light. The single grain of augite at the bottom of the image forms three-grain junctions with the plagioclase grains, all of which are defined by the pseudomorphing of the previously melt-filled pore by the augite, with little or no corresponding inwards growth of the plagioclase (three examples are marked by asterisks). Scale bar is 200 μm long. **b** Sample ROM48-219 from the Traigh Bhàn na Sgùrra sill, Isle of Mull (previously described by Holness et al. (2012b)), photographed under plane polarised light. The two arrowed three-grain junctions are formed by the pseudomorphing of the previously melt-filled pore corner by augite. The two junctions between plagioclase grains marked by the white asterisks are filled with glassy mesostasis, instead of augite. The tendency of augite to fill the wider junctions means that the median value of the augite–plagioclase–plagioclase dihedral angle population is higher

than 60° . Scale bar is 200 μm long. **c** Sample 87–110, from the centre of the 128 m thick Portal Peak sill, Antarctica (previously described by Holness et al. 2012b), photographed under plane polarised light. The three-grain junctions are characterised by curvature of the two augite–plagioclase boundaries, denoting simultaneous growth of the plagioclase walls and augite into the pore (three examples are marked by asterisks). The curvature is asymmetric for the junctions shown in this image, but more generally it is symmetric in this sample. Scale bar is 200 μm long. **d** Sample 458242 from Lower Zone of the Layered Series of the Skaergaard Intrusion, photographed under plane polarised light. The arrowed three-grain junction shows the highly asymmetric geometry typical of augite–plagioclase–plagioclase junctions in gabbroic layered intrusions. The trace of the (010) twins in the two plagioclase grains are shown by black lines. Scale bar is 1 mm long

values of Θ_{cpp} of 79.5° and 94.5° , and a dolerite from the Basement Sill, Antarctica, with a reported Θ_{cpp} of 100° (all previously described by Holness et al. 2012b).

For an investigation of the effects on 3-grain junction geometry of the extent to which cumulates are ad- or orthocumulate, we re-examined previously described samples from the Rum Eastern Layered Intrusion and the Skaergaard Intrusion. Our choice was determined by the need to examine representative samples of gabbros for comparison with troctolites containing variable amounts of interstitial material. The variable extent to which fabrics are present in the suite of chosen samples is not thought to be significant, as Holness (2010) showed that the median value of the (true 3D) dihedral angle is the same within uncertainty for sections cut perpendicular and parallel to foliation.

The Rum Eastern Layered Intrusion comprises peridotitic, troctolitic and gabbroic cumulates (Emeleus

1997). For this study, we examined troctolites from Unit 12 and gabbros from Unit 9. The troctolites have previously been described by Holness and Winpenny (2009) who reported the augite–plagioclase–plagioclase dihedral angles (with more detailed measurements reported by Holness et al. 2013). The gabbroic cumulates were previously described by Holness et al. (2007), with dihedral angles reported by Holness et al. (2013). The Rum troctolites are strongly adcumulate, with augite forming rare, small, interstitial grains and thin rims separating cumulus olivine from the surrounding cumulus plagioclase. The gabbros are also strongly adcumulate and are dominated by olivine, plagioclase and augite, with almost undetectable amounts of more evolved phases such as Fe–Ti oxides and apatite. Both gabbros and troctolites from Rum commonly have a pronounced igneous fabric defined by the preferred alignment of cumulus plagioclase. We chose two troctolites and two gabbros

Table 1 Details of troctolitic (plain text) and gabbroic (bold text) cumulates, presented in order of increasing volume of interstitial minerals

Sample	Θ_{cpp}	Mineral mode (vol.%)					Volume % liquid		Mean absolute $\Delta\phi$	Mean proportional $\Delta\phi$
		Plag	Olivine	Augite	Low-Ca pyroxene	Fe–Ti oxides	From modes	P_2O_5		
R12-J5	79±4	81.0	18.0	1.0	–	–	2.9–3.3		16.1	26.7
R12-J13	82.5±4	87.0	10.0	3.0	–	–	8.6–9.8		23.6	33.5
R12-J13									<i>35.1</i>	<i>46.3</i>
949'11"	85.5±4	81.2	13.9	1.8	2.3	0.7	11.8–13.6	48	26.9	33.0
571'4"	80.5±3	88.3	5.5	2.0	3.0	1.2	15.5–18.6	46	27.6	35.0
661'2"	96±1.5	79.7	12.3	4.2	2.7	1.1	17.0–19.8	24	33.2	38.2
371'7"	82±4	71.8	18.9	6.2	2.8	0.3	18.6–19.0	37	28.6	38.4
930'2"	82±5	80.6	8.0	6.7	3.1	1.7	22.8–26.9	54	33.9	46.3
458220	100±2.5	84.0	3.1	7.4	4.3	1.2	26.0–28.9	29	44.3	52.4
1049'11"	83.5±3.5	78.8	8.1	5.3	7.2	0.6	30.8–32.2	63	37.6	50.2
1070'2"	77±3	77.3	7.0	10.8	2.5	2.4	34.4–37.3		46.2	57.5
987'11"	84.5±5	70.4	12.2	15.1	1.9	0.4	42.2–46.4		27.2	32.3
621'1"	92±4	74.1	7.5	15.6	2.7	0.2	43.7–47.1	27	37.9	44.9
458212	83.5±4	65.9	12.1	13.2	6.5	2.3	41.8–47.1	35	38.5	54.8
458213	83.5±2	65.7	6.1	20.1	7.0	1.1	56.9–59.6	42	38.0	38.4
1091'6"	79±3.5	70.9	3.8	23.8	1.2	0.3	63.7–71.1	23	40.9	55.1
F11	91±1.5								38.7	46.8
F12	90±2								38.7	47.2
458231	100±2								42.9	53.4
458226	97±2								41.0	47.8

Those with prefix R12 or F are from the Rum Eastern Layered Intrusion, those beginning 458 are Skaergaard Layered Series samples described by Tegner et al. (2009) while the remainder are from the Skaergaard Layered Series as sampled by the Cambridge drill core (Holness et al. 2015) with the sample number giving the depth in the core in feet and inches. The previously reported median augite-plagioclase-plagioclase dihedral angle is given by Θ_{cpp} (reported by Holness et al., 2007; 2013) and Holness & Winpenny (2009). Plagioclase and olivine are primocryst phases in the troctolites, and the remaining phases are interstitial. The method of calculating the volume % interstitial liquid using the mineral modes is described in the text. The values of volume % liquid calculated using the bulk rock P_2O_5 concentration were presented by Tegner et al. (2009) for the samples prefixed by 458, and were calculated using the same method for the remaining samples from the bulk rock P_2O_5 presented by Holness et al. (2013). The values of $\Delta\phi$ for R12-J13 written in italics are those for olivine–plagioclase–plagioclase junctions

from Rum (mineral modes and dihedral angles are presented in Table 1).

The lower part of the Layered Series of the Skaergaard Intrusion comprises troctolitic orthocumulates (denoted Lower Zone a, or LZa; Wager and Brown 1968) overlain by gabbroic orthocumulates (denoted Lower Zone b, or LZb; Wager and Brown 1968). The troctolites contain abundant interstitial augite, orthopyroxene (inverted pigeonite), Fe–Ti oxides and apatite, with rare pockets of granophyre. The gabbroic cumulates also contain these interstitial minerals, with the exception of augite which is part of the cumulus assemblage. There is no strong fabric in any of the samples examined here. The mineral modes have been reported by Holness et al. (2013, 2015) and by Tegner et al. (2009), and dihedral angles by Holness et al. (2013, 2015), and are presented in Table 1. We chose two gabbros and 13 troctolites from Skaergaard, ensuring a wide range of troctolites from strongly adcumulate rocks to orthocumulates.

Analytical methods

Amount of interstitial liquid in the cumulates

The amount of liquid retained in the crystal mush during cumulate solidification, commonly called “trapped liquid”, is generally calculated using the bulk rock concentration of P_2O_5 (e.g. Tegner et al. 2009). Previously published values of trapped liquid for a subset of the Skaergaard troctolites are presented in Table 1 (from Tegner et al. 2009) together with values calculated for the remainder of the Skaergaard troctolites using the method of Tegner et al. (2009).

For comparison with the values of liquid calculated using bulk rock P_2O_5 , we used the mode of interstitial material in the troctolitic cumulates to estimate the amount of pore space present in the mush at the moment adcumulus overgrowth of the primocrysts ceased and the interstitial phases began to grow. For the particular case of the Skaergaard cumulates, this moment is when further overgrowth of

olivine and plagioclase primocrysts is accompanied by the nucleation and growth in the interstitial spaces of augite, orthopyroxene (via reaction of olivine), oxides, apatite, and finally granophyre: for the samples considered here, the volumetric proportions of biotite, apatite and granophyre are sufficiently low (< 1 volume %) to be disregarded. If we assume that oxides begin to crystallise before significant reaction of the olivine to form pigeonite, the relevant reactions for crystallisation of the interstitial liquid in the Skaergaard cumulates are:

- (1) Liquid = olivine + plagioclase + augite,
- (2) Liquid = olivine + plagioclase + augite + oxides,
- (3) Liquid + olivine = plagioclase + augite + low-Ca pyroxene (+ oxides)

The experimental results of Thy et al. (2006) suggest that reaction 1 begins at 1168 ± 5 °C, reaction 2 begins at 1102 ± 5 °C, and orthopyroxene begins to crystallise between 1084 °C and 1093 °C (reaction 3). The weight proportions of the phases produced by each reaction are given in Table 2, together with the published source. There is no published information that lets us include oxides as a crystallising phase in reaction 3 so it was ignored. To constrain the stoichiometry of reaction 2, we used the modal compositions for the five LZc rocks described by Tegner et al. (2009) that contain virtually no low-Ca pyroxene and are therefore effectively adcumulate. Since Tegner et al. (2009) collected only average gabbros (avoiding melanocratic and leucocratic layers), it is likely that these rocks contain close-to-cotectic proportions of the different phases. However, two of the five adcumulate samples are relatively poor in oxides so we split them into two groups to bracket the true stoichiometry of reaction 2 (Table 2).

The first step in calculating the amount of liquid solidified in the cumulate is the removal of low-Ca pyroxene from the bulk compositions given in Table 1, together with appropriate quantities of the other phases according to reaction 3 (Table 2; we used densities (in units of 10^3 kg m^{-3}) of 2.7, 3.3, 3.4, 3.5 and 5.2 for plagioclase, olivine, low-Ca pyroxene, augite and oxides respectively, to convert from weight

% to volume %). There is insufficient augite in a few samples to account for the observed mode of low-Ca pyroxene: for these rocks, so we set the mode of augite to zero for the second and third steps. Next, oxides were removed, together with appropriate quantities of the other phases according to reaction 2. Finally, any remaining interstitial augite was removed together with appropriate quantities of olivine and plagioclase according to reaction 1. The volume fraction of liquid corresponding to the lost solid material was calculated assuming a liquid density of $2.65 \times 10^3 \text{ kg m}^{-3}$, providing an indication of the amount of liquid present in the crystal mush at the moment the interstitial minerals began to grow. We applied the same process to the 2 troctolites from Rum: although the liquid line of descent for the Rum magma is rather different (there is no evidence for reaction 3, for example), there is so little interstitial material in these adcumulates (Table 1) that only augite removal (via reaction 1) is possible, thus minimising any inaccuracies in our treatment. The maximum and minimum values of the calculated liquid fraction are given in Table 1: the maximum value resulted from a combination of the Toplis and Carroll (1995) reaction 1 and a reaction 2 stoichiometry derived from the more plagioclase-rich LZc samples (Table 2).

Three-grain junction geometry

We used a Leitz 4-axis universal stage mounted on a James Swift polarising microscope with a $\times 32$ long working distance objective, permitting the measurement of the true 3D values of angles between grain boundaries with uncertainties of a few degrees (see Holness (2010) for a brief guide on the technique). For the three dolerite samples, we measured the true value of the augite–plagioclase–plagioclase dihedral angle, together with the angle between the two augite–plagioclase grain boundaries created by the original impingement of the two plagioclase grains, for between 31 and 100 individual junctions. For the suite of troctolites and gabbros from Rum and Skaergaard, we measured between 30 and 50 individual augite–plagioclase–plagioclase junctions in each sample, noting the angle between the extension of the plagioclase–plagioclase grain boundary and the two

Table 2 Stoichiometry (in wt.%) for the three reactions used to determine the liquid fraction required to account for the observed modes of interstitial phases

	Olivine	Plagioclase	Augite	Oxides	Low-Ca pyroxene	Source literature
Reaction (1)	0.09	0.46	0.45	–	–	Thy et al. (2006)
	0.12	0.48	0.40	–	–	Toplis and Carroll (1995)
Reaction (2)	0.18	1.7	1.1	1 (67% ilmenite)	–	Leuco-accumulates in LZc (Tegner et al. 2009)
	0.15	0.41	0.4	1 (64% ilmenite)	–	Melano-accumulates in LZc (Tegner et al. 2009)
Reaction (3)	–0.10	0.40	0.40	–	0.20	Thy et al. (2006)

augite–plagioclase grain boundaries. For a completely symmetric three-grain junction these two angles are the same, whereas for an eagle’s beak they differ significantly. We report the mean of the absolute difference in these angles, and the mean of the proportional difference relative to the overall dihedral angle (Table 1). Given that the extent of asymmetry at any one junction may vary with the magnitude of the dihedral angle at that junction, we endeavoured to ensure our choice of three-grain junctions within any sample resulted in the same median dihedral angle as reported by the earlier studies (Table 1).

Results

There is no correlation between the volume of interstitial liquid calculated using the bulk rock concentration of P_2O_5 and the mineral modes in the troctolites (Table 1, Fig. 3), in agreement with the conclusions of McBirney and Hunter (1995) and Holness et al. (2020). Indeed, one of the highest values of calculated interstitial liquid is found in sample 949’11”, which contains only 4.8 vol.% interstitial minerals, and is clearly strongly adcumulate in nature. This suggests that calculations of liquid content based only on the bulk rock P_2O_5 are unreliable, due perhaps to the migration of interstitial liquids during solidification (Karykowski and Maier 2017), or to the crystallisation of apatite in channels through which late-stage liquids flowed (Meurer and Meurer 2006).

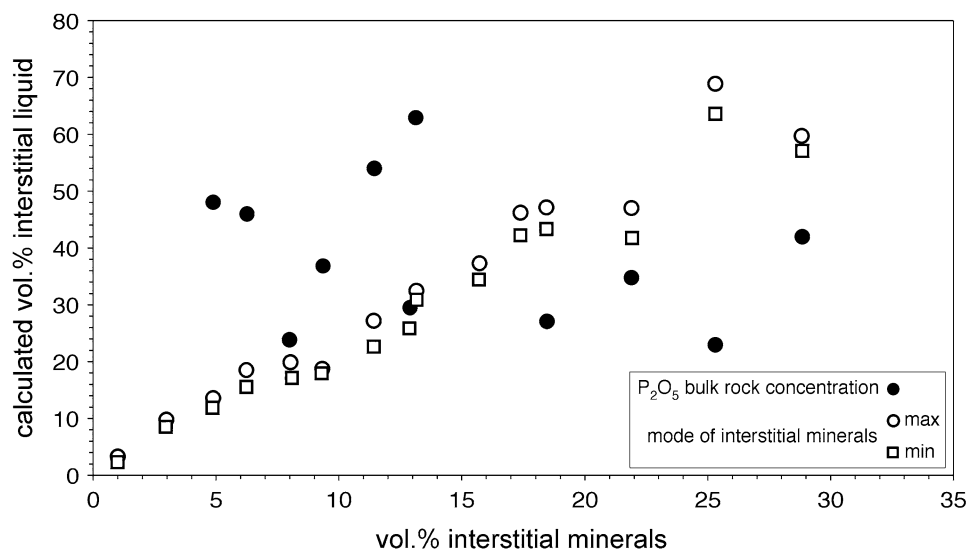
In contrast to the results using bulk rock concentration of P_2O_5 , there is an (as expected) strong correlation between the mode of interstitial minerals and the calculated amount of interstitial liquid present in the mush at the moment adcumulus growth ceased (Table 1, Fig. 3). The maximum

amount of liquid in the troctolite, calculated from modes, is ~60 vol.%, consistent with estimates of mush porosity based on random loose packing of non-spherical particles and clusters (Campbell 1978; Philpotts and Dickson 2000). These calculated liquid volumes are likely to bear some relevance to the extent of adcumulus growth because there is also a strong correlation between the mineral modes (and hence the amount of interstitial liquid) and the geometry of 3-grain junctions (Fig. 4).

Our observations of the geometry of augite–plagioclase–plagioclase junctions lead to two main results. The first of these highlights the importance of the amount of interstitial liquid present in the (plagioclase-dominated) mush when significant growth of augite begins. The extent of asymmetry of the three-grain junctions, measured using the average values of either the absolute, or the relative, difference between the two angles formed by the extension of the plagioclase–plagioclase grain boundary (Table 1; see inset in Fig. 4), increases steadily as the troctolites depart further from adcumulates until the mode of interstitial phases reaches about 12 vol.%. The amount of liquid in the plagioclase + olivine mush that corresponds to this amount of interstitial material is ~30 vol.% (Table 1). At this point, the extent of asymmetry remains essentially constant and indistinguishable from that in gabbroic cumulates (Fig. 4). Three-grain junctions are thus relatively symmetrical in strongly adcumulate troctolites, being mainly of the first two types of junction (with the balance between the two dependent on cooling rate), but become more asymmetric (eagles’ beaks) as the troctolites gain more orthocumulate character.

The one exception to the constant amount of asymmetry for troctolite containing > 12% volume interstitial minerals is provided by sample 987’ 11”, in which three-grain junctions are relatively symmetric. In this sample, the

Fig. 3 The volume % of liquid in the plagioclase + olivine primocryst framework shown as a function of the mode of interstitial minerals (augite, orthopyroxene and Fe–Ti oxides), calculated either from the mode of interstitial minerals, or from the bulk rock P_2O_5 concentration. There is no correlation between the two methods of calculating the volume % of interstitial liquid. Data presented in Table 1



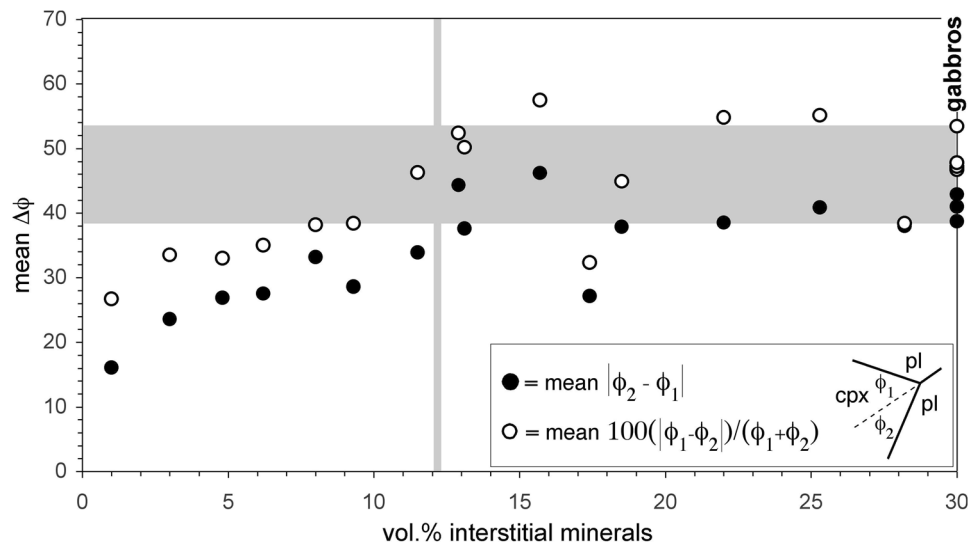


Fig. 4 The mean difference in the two angles created by the extension of the plagioclase–plagioclase grain boundary (see inset cartoon) as a function of the volume of interstitial minerals in troctolitic cumulates from Rum and Skaergaard. The horizontal grey box gives the range of mean differences seen in gabbro (with the data from the four gabbro samples presented in Table 1 shown on the right-hand axis): with

the exception of one sample (Skaergaard troctolite 987'11" at 17.4% volume interstitial minerals), three-grain junctions in troctolites have a similar asymmetry to those in gabbros if the volume of interstitial minerals in the troctolite exceeds ~ 12 vol.% (shown by the vertical grey box)

orientation of the plagioclase–plagioclase grain boundary is rotated within a few tens of microns from the three-grain junction so that it meets the two augite–plagioclase grain boundaries at a more symmetric angle: such rotation was not seen in other samples examined during this study and is suggestive of a limited approach to textural equilibrium. Sample 987' 11" lies immediately above a positive excursion in Θ_{cpp} that has been attributed to a major influx of magma into the inflating chamber, with a consequent slowing of the cooling rate (Holness et al. 2015). Such a slowing is likely to be associated with (sub-solidus) textural equilibration of three-grain junctions in horizons both immediately above and below that marking the influx.

The second result pertains to the three dolerite samples. We find that, in general, the (true, 3D) augite–plagioclase–plagioclase dihedral angle is similar to that of the (true, 3D) angle subtended by the two impinging plagioclase growth faces if that original angle at the pore corner is large (Fig. 5). If the original angle at the pore corner is small, then there is a commensurately greater difference between the original angle and the final dihedral angle. Most significantly, the dihedral angles at individual 3-grain junctions only rarely exceed the median value of the population of fully equilibrated angles (109° ; Holness et al. 2012a), even in sample 87–89 which has Θ_{cpp} close to the minimum value of 78° , in which textural equilibration is likely to have been minimal (Fig. 5).

Discussion and conclusions

In the companion paper, we attempt to account for the two results presented here. We present a simple geometric theory of three-grain junction formation for which the fundamental controls on the geometry are the relative rates of growth of augite and plagioclase into a pore created by the meeting of two plagioclase grains (examples in Figs. 1b and c are marked by asterisks). This simple model, based on the concept of Holness (2015), accounts for the formation of the first and second types of three-grain junction. Importantly, however, we find that the rate of crystal growth during the last stages of pore filling to form the junction is modified by an increasing importance of interfacial energy as the remaining melt volume at the nascent three-grain junction approaches zero. This increasing control by interfacial energy is analogous to that in classical nucleation theory, in which embryos only become stable once the free energy decrease associated with the solidification reaction becomes larger than the free energy increase associated with the formation of the solid–liquid interface (Volmer and Weber 1926). We find that this accounts for our otherwise perhaps surprising finding that augite–plagioclase–plagioclase dihedral angles formed during solidification only rarely exceed the equilibrium value (the median value of which is 109° (Holness et al. 2012a), although there is some spread around this value due to anisotropy) (Fig. 5), and demonstrates some control by interfacial energies on the final three-grain geometry, even in rapidly cooled samples.

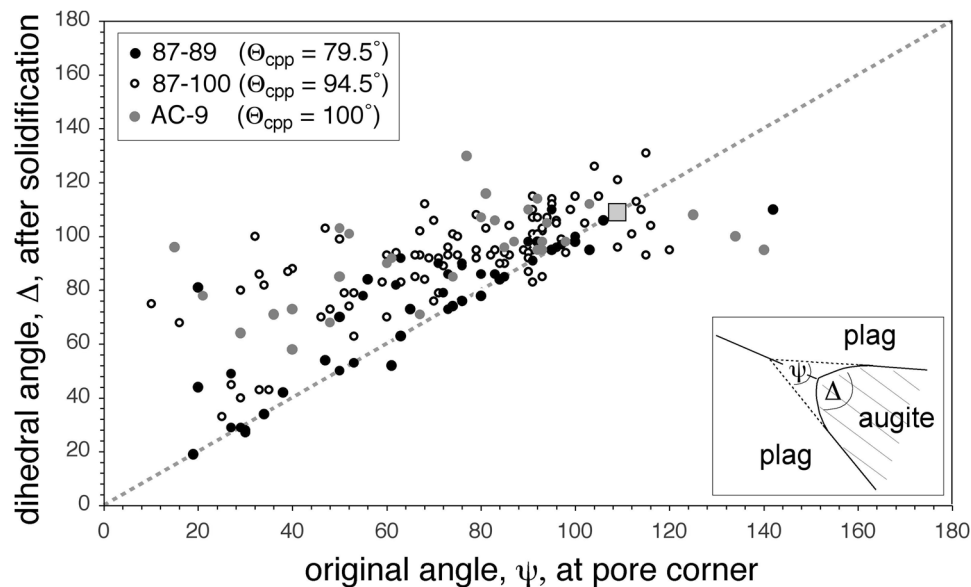


Fig. 5 Comparison of the angle (ψ) subtended by the impinging growth faces of the 2 plagioclase grains far from the dihedral angle and the dihedral angle itself (Δ) for populations of 3-grain augite-plagioclase-plagioclase junctions in three samples of dolerite with varying median dihedral angles (Θ_{cpp} —values are shown in the text box in the figure); the units of both axes are degrees. All angles were measured using a universal stage, and are thus the true angle in 3D. The dotted line shows the 1:1 correlation expected for perfect pseu-

domorphing by augite of a melt-filled pore corner created by the impingement of two plagioclase grains. Samples 87–89 and 87–100 are from the Portal Peak sill, Antarctica, and AC-9 is from the Basement sill, Antarctica. Both bodies are formed of dolerite with randomly oriented plagioclase, and these three samples have been previously described by Holness et al. (2012b). The grey square shows the median value of the population of equilibrium augite-plagioclase-plagioclase dihedral angles (109° Holness et al. 2012a)

Our examination of three-grain junction geometry as a function of mineral mode in troctolites shows that the third type of junction, the eagle's beak, is associated with a large volume of interstitial liquid in the plagioclase framework at the cessation of adcumulus growth. In the companion paper, we argue that eagles' beaks form if the two plagioclase grains impinge only once augite growth has progressed significantly into the pore space (examples are marked by an "o" in Figs. 1b, 1d). A schematic representation of this process is shown in Fig. 6.

A simple test of the hypothesis that eagles' beaks result from the simultaneous growth of plagioclase and the second mineral phase (i.e. augite) to form a bi-mineralic framework is provided by the Rum adcumulate troctolite R12-J13. The augite-plagioclase-plagioclase three-grain junctions in this sample are generally symmetrical, consistent with significant growth of augite only after the formation of the original crystal framework (consisting of plagioclase and olivine) (Table 1). However, the three-grain junctions between the two *primocryst* phases, olivine and plagioclase, are significantly asymmetric, similar to augite-plagioclase-plagioclase junctions in gabbros (Table 1). In contrast to the augite-plagioclase-plagioclase junctions, which were created by augite growth within an existing plagioclase (+ olivine) crystal framework, the olivine-plagioclase-plagioclase junctions are likely to have been formed predominantly

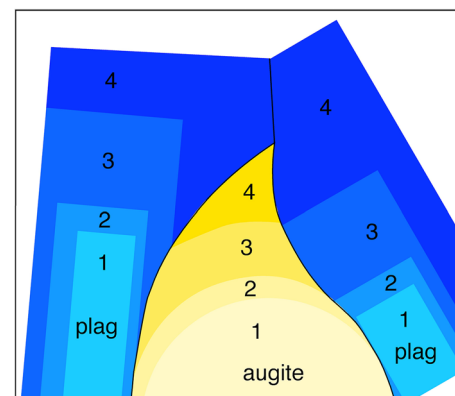


Fig. 6 A schematic representation of the formation of an eagle's beak three-grain junction geometry. The augite grows in a space bounded by two plagioclase grains (plag) which do not touch each other until a late stage in the development of the three-grain junction. The successive growth stages are numbered sequentially, with a progressively darker shade of yellow (augite) or blue (plagioclase). The augite initially impinges on the right-hand plagioclase grain at stage 1, and impinges on the left-hand grain at stage 2. When the augite grain reaches the corner of the right-hand grain at the end of stage 2, it becomes temporarily locked to the corner, resulting in a changing sense of curvature of the developing augite-plagioclase grain boundary. Further details are given in the companion paper

during the earliest stages of mush solidification, when the two framework-forming minerals olivine and plagioclase were growing simultaneously (c.f. Figure 6), resulting in relatively late impingement of the two plagioclase grains in an analogous manner to that seen in strongly orthocumulate troctolites and gabbros. Hence the olivine junctions are more likely to be eagles' beaks, whereas the augite junctions are symmetrical.

The geometry of augite–plagioclase–plagioclase three-grain junctions in mafic rocks is thus a function not only of cooling rate, but also of the progression along the liquid line of descent during fractionation. The first junction type is formed in rapidly cooled rocks, while the other two types are found in more slowly cooled bodies. In these larger plutonic bodies, type two junctions are formed in relatively primitive liquids, in which the crystal mushes on the intrusion margins are formed predominantly of plagioclase and olivine, whereas type three junctions, the eagles' beaks, form once augite comprises an important component of the crystal framework in the accumulating mush, either because it is a framework-forming primocryst phase or because it grows from highly abundant interstitial liquid in which nucleation and growth of augite occurs before the plagioclase framework is complete. Hence, as the amount of interstitial liquid increases in a troctolitic mush, the style of junction formation tends towards that observed in gabbros. In the companion paper, we therefore develop our simple geometric model to include consideration of variation in the timing of impingement of the two plagioclase grains.

Acknowledgements A.C.F. acknowledges the support of the Mathematics Applications Consortium for Science and Industry (www.macsi.ul.ie) funded by the Science Foundation Ireland mathematics grant 12/IA/1683, and EPSRC grant no EP/K032208/1. M.B.H. acknowledges the support of the Natural Environment Research Council (grant number NE/N009894/1). The authors would like to thank the Isaac Newton Institute for Mathematical Sciences, Cambridge, for support and hospitality during the programme 'Melt in the mantle' where work on this paper was undertaken. Helpful comments of two anonymous reviewers led to significant improvements of an earlier version of the manuscript.

Open Access This article is licensed under a Creative Commons Attribution 4.0 International License, which permits use, sharing, adaptation, distribution and reproduction in any medium or format, as long as you give appropriate credit to the original author(s) and the source, provide a link to the Creative Commons licence, and indicate if changes were made. The images or other third party material in this article are included in the article's Creative Commons licence, unless indicated otherwise in a credit line to the material. If material is not included in the article's Creative Commons licence and your intended use is not permitted by statutory regulation or exceeds the permitted use, you will need to obtain permission directly from the copyright holder. To view a copy of this licence, visit <http://creativecommons.org/licenses/by/4.0/>.

References

- Cahn JW (1980) Surface stress and the chemical equilibrium of small crystals: I. The case of the isotropic surface. *Acta Metall* 28:1333–1338
- Campbell IH (1978) Some problems with cumulus theory. *Lithos* 11:311–323
- Emeleus CH (1997) *Geology of Rum and the adjacent islands*. Memoir for 1:50 000 Geological Sheet 60 (Scotland). HM Stationery Office, London
- Holness MB (2010) Decoding dihedral angles in melt-bearing and solidified rocks. *J Virtual Explorer* 35. <https://doi.org/10.3809/jvirtex.2010.00265>
- Holness MB (2014) The effect of crystallization time on plagioclase grain shape in dolerites. *Contrib Miner Petrol* 168:1076. <https://doi.org/10.1007/s00410-014-1076-5>
- Holness MB (2015) Plagioclase growth rates control three-grain junction geometry in dolerites and gabbros. *J Petrol* 56:2117–2144
- Holness MB, Winpenny B (2009) The Unit 12 allivalite, Eastern Layered Intrusion, Isle of Rum: a textural and geochemical study of an open-system magma chamber. *Geol Mag* 146:437–450
- Holness MB, Hallworth MA, Woods A, Sides RE (2007) Infiltration metasomatism of cumulates by intrusive magma replenishment: the Wavy Horizon, Isle of Rum, Scotland. *J Petrol* 48:563–587
- Holness MB, Humphreys MCS, Sides R, Helz RT, Tegner C (2012a) Towards an understanding of disequilibrium dihedral angles in mafic rocks. *J Geophys Res*. <https://doi.org/10.1029/2011JB008902>
- Holness MB, Richardson C, Helz RT (2012b) Disequilibrium dihedral angles in dolerite sills: a new proxy for cooling rate. *Geology* 40:795–798
- Holness MB, Namur O, Cawthorn RG (2013) Disequilibrium dihedral angles in layered intrusions: a microstructural record of fractionation. *J Petrol* 54:2067–2093
- Holness MB, Tegner C, Namur O, Pilbeam L (2015) The earliest history of the Skaergaard magma chamber: a textural and geochemical study of the Cambridge Drill Core. *J Petrol* 56:1199–1227
- Holness MB, Tegner C, Nielsen TFD, Charlier B (2017) The thickness of the mushy layer on the floor of the Skaergaard magma chamber at apatite saturation. *J Petrol* 58:909–932
- Holness MB, Morris C, Vukmanovic Z, Morgan DJ (2020) Insights into magma chamber processes from the relationship between fabric and grain shape in troctolitic cumulates. *Front Earth Sci* 8:352. <https://doi.org/10.3389/feart.2020.00352>
- Karykowski BT, Maier WD (2017) Microtextural characterisation of the lower zone in the Western limb of the Bushveld Complex, South Africa: evidence for extensive melt migration within a sill complex. *Contrib Miner Petrol* 172:60
- McBirney AR, Hunter RH (1995) The cumulate paradigm reconsidered. *J Geol* 103:114–122
- Meurer WP, Meurer MES (2006) Using apatite to dispel the “trapped liquid” concept and to understand the loss of interstitial liquid by compaction in mafic cumulates: an example from the Stillwater Complex, Montana. *Contrib Miner Petrol* 151:187–201
- Morse SA (2011) The fractional latent heat of crystallizing magmas. *Am Miner* 96:682–689
- Philpotts AR, Dickson LD (2000) The formation of plagioclase chains during convective transfer in basaltic magma. *Nature* 406:59–61
- Philpotts AR, Shi J, Brustman C (1998) Role of plagioclase crystal chains in the differentiation of partly crystallised basaltic magma. *Nature* 395:343–346
- Philpotts AR, Brustman CM, Shi J, Carlson WD, Denison C (1999) Plagioclase-chain networks in slowly cooled basaltic magma. *Am Miner* 84:1819–1829

- Tegner C, Thy P, Holness MB, Jakobsen JK, Leshner CE (2009) Differentiation and compaction in the Skaergaard intrusion. *J Petrol* 50:813–840
- Thy P, Leshner CE, Nielsen TFD, Brooks CK (2006) Experimental constraints on the Skaergaard liquid line of descent. *Lithos* 92:154–180
- Toplis MJ, Carroll MR (1995) An experimental study of the influence of oxygen fugacity on Fe–Ti oxide stability, phase relations, and mineral–melt equilibria in ferro-basaltic systems. *J Petrol* 36:1137–1170
- Voll G (1961) New work on petrofabrics. *Geol J* 2:503–567
- Volmer M, Weber A (1926) Keimbildung in übersättigten Gebilden. *Z Phys Chem* 119U:227–301
- Wager LR, Brown GM (1968) Layered igneous rocks. Oliver and Boyd, Edinburgh

Publisher's Note Springer Nature remains neutral with regard to jurisdictional claims in published maps and institutional affiliations.